41st AIAA/ASME/SAE/ASEE **AIAA-2005-3578**
Joint Propulsion Conference and Exhibit
Tucson, Arizona, 10 - 13 Jul 2005

Pattern Factor Sensing and Control Based on Diode Laser Absorption

Tudor I. Palaghita* and Jerry M. Seitzman†
Georgia Institute of Technology,
Daniel Guggenheim School of Aerospace Engineering,
Atlanta, GA, 30332

This paper describes the development and demonstration of a sensor for pattern factor control based on diode laser line-of-sight water absorption. Temperature nonuniformity is characterized in two ways: by defining a nonuniformity variable based on the difference in temperatures measured with two pairs of absorption lines, as well as by using several absorption lines to describe the temperature distribution. The nonuniformity variable is shown to track the mixedness of the flow. Preliminary experimental measurements of temperature nonuniformity in a temperature-stratified combustor exhaust using an external cavity diode laser are shown. Simulations of sensor operation based on combustor temperature and concentration data from CFD simulations are used to analyze the problems encountered in the experiments. Solutions to errors introduced by changing correlation between the temperature and species fields, the inability to fast scan over multiple lines, and noise are presented based on the simulations.

I. Introduction

The ongoing drive for better performance, reduced emissions, and lower maintenance costs for gas-turbine engines requires higher levels of control to be employed at all levels of operations. Sensor development, especially in the hot gas and reacting flow regions can be a key enabler for many intelligent engine control systems. Sensing becomes especially important at off-design operation and as engines age.

Pattern factor (temperature distribution) sensing has the potential to enable improved combustors with better mixing control, increased uniformity between injectors, and higher average temperatures, yielding increased engine performance. Furthermore, the life of the turbine blades can also be increased by controlling the combustor exit temperature profile, and mixing control may improve emissions characteristics. Pattern factor (PF), typically defined as in Eq. (1) below, is a measure of the peak deviation from the mean of the combustor exit temperature profile ($\overline{T_4}$).

$$PF = \frac{T_{4,\max} - \overline{T_4}}{\overline{T_4}} \tag{1}$$

It may be considered an indicator of the maximum thermal loading of the turbine blades and vanes; a large PF value affects both the efficiency of the engine (forcing lower average combustor temperatures) and the life of the turbine vanes and blades.

*Graduate Research Assistant, School of Aerospace Engineering, AIAA Student member
†Associate Professor, School of Aerospace Engineering, AIAA Associate Fellow

Optical sensors generally provide unique capabilities for sensing hot flow properties. Lasers in particular have proved extremely useful in the development of combustion sensors, as they are rugged, non-intrusive, fast, and can be used in conjunction with fiber-optics to locate the sensor remotely.

Although diode lasers are already a well-established technology, new improvements in power, tunability, and access to new wavelengths allow for new sensor applications, keeping diode lasers very much in the arena of active research. Diode lasers are also relatively inexpensive, widely available, have a fast response time, wide tuning bandwidth, narrow spectral features, and sufficient power to provide sensors with good sensitivity. Diode-laser sensors for temperature, pressure, species concentration, and velocity based on absorption spectroscopy have been demonstrated for laboratory and in-situ combustion systems.[1-5] Usually the laser is tuned over one or more spectral features and the resulting absorption is used to compute flow properties of interest.

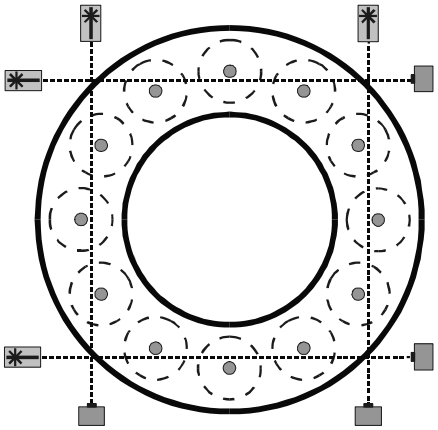

Figure 1. Gas-turbine annular combustor exit plane instrumented for pattern factor sensing.

This paper describes the continued development and testing of a diode-laser, direct absorption sensor for temperature nonuniformity. Three or more water transitions are probed with a diode laser; the ratio of absorbances of each pair of transitions yields a line-of-sight average temperature based on the Boltzman fraction of the absorbers. When the gas properties (temperature, absorber mole fraction) are uniform, any such pair would yield essentially the same temperature. When the gas properties change along the line of sight, because each line has a different nonlinear dependence on temperature and concentration, different line-pairs will yield different "average" temperatures. A nonuniformity parameter "U" is defined based on two of these “average” temperatures. *U* approaches zero when the line-of-sight temperature is uniform and increases as it becomes more nonuniform. Other ways to characterize this nonuniformity are also described below. An analysis of the usefulness of *U* and factors affecting sensor performance is performed through simulations of the sensor operation. Preliminary experimental results are shown for sensing the exit temperature profile of a temperature stratified methane-air combustor.

For the current sensor implementation, water was chosen as the marker species because it is a major combustion product that has relatively strong absorption lines throughout a large portion of the spectrum. Moreover, it is easy to find water lines with little or no interference from other combustion products. The rotational-vibrational transitions used in the experiments (between 1950 and 2030nm) were chosen based on the available laser hardware. The same methodology can be used at other wavelengths and with other species based on available lasers.

The primary application for this sensor is circumferential pattern factor sensing and control in an annular combustion rig (Fig. 1). For example, using a few of these sensors, the whole circumferential temperature profile can be characterized (and therefore related issues such as nonuniformities between injectors, problems with specific injectors, and mixing issues) and controlled. Furthermore, the same sensor concept can be used in large arrays of industrial burners and other manufacturing applications where temperature uniformity is essential for certain chemical processes.

II. Absorption Theory

The narrowband absorption of a light signal at wavelength ν (cm^{-1}) with incident intensity I_0 and transmitted intensity I by a medium of thickness L (cm), is described by the Beer-Lambert Law:

$$\frac{I}{I_0}(\nu) = e^{\int_0^L -pxS_i(T)\phi(\nu-\nu_0,T,x,p)dl} \tag{2}$$

where p is the pressure (atm), x is the absorber mole fraction, S is the line strength (cm^{-2} atm^{-1}) of the i^{th} transition (centered at ν_0), T is the temperature (K), and ϕ is the line shape function (cm) whose integral is normalized to unity. For a particular transition i centered at $\nu_{0,i}$, the line strength S is a function of temperature only:

$$S_i(T) \approx S_i(T_0)\frac{Q(T_0)}{Q(T)}\frac{T_0}{T}\exp\left(-\frac{hcE''}{k}\left(\frac{1}{T}-\frac{1}{T_0}\right)\right)\cdot\left[1-\exp\left(\frac{-hc\nu_{0,i}}{kT}\right)\right]\cdot\left[1-\exp\left(\frac{-hc\nu_{0,i}}{kT_0}\right)\right]^{-1} \quad (3)$$

where Q is the partition function, E'' is the lower state energy of the transition (cm^{-1}), h is Plank's constant, c is the speed of light, and k is Boltzman's constant. T_0 is a reference temperature, taken here to be 296K, consistent with the HITRAN[6] database. The last two terms account for the effect of stimulated emission and can generally be neglected at wavelengths below 2.5 μm and temperatures below 2500 K.

In a medium with uniform properties (temperature and concentration), one can determine the temperature and mole fraction of the species of interest by probing two absorption lines. By integrating over a frequency band centered at ν_0, the line shape function is eliminated and the ratio R of the absorbances of two lines becomes a function of temperature only:

$$abs_i = \int_{-\infty}^{\infty} -\ln\left(\frac{I}{I_0}(\nu)\right)d\nu = \int_{-\infty}^{\infty}\int_0^L p\cdot x\cdot S_i(T)\phi_i(\nu-\nu_0,T,x,p)dld\nu = pxS_i(T)L \quad (4)$$

$$R_{ij} = \frac{abs_i}{abs_j} = \frac{S_i(T)}{S_j(T)} = \frac{S_i(T_0)}{S_j(T_0)}\exp\left(-\frac{hc}{k}(E_i''-E_j'')\left(\frac{1}{T}-\frac{1}{T_0}\right)\right) \quad (5)$$

Using the absorbance of two lines one can determine the temperature of the gas using Eq. (5) and the concentration of the species of interest using Eq. (4). In this gas with uniform properties, any two lines we pick would yield the same results (neglecting experimental errors).

A. Nonuniform flow properties

When the temperature and concentration of the medium are not uniform, as is generally the case in a combustor, the integral in Eq. (4) cannot be solved without prior knowledge of either the temperature or concentration profiles. For arbitrary temperature and concentration profiles along the line of sight, the ratio of the absorbances of 2 lines i and j becomes:

$$R_{ij} = \frac{abs_i}{abs_j} = \frac{\int_0^L xS_i(T)dl}{\int_0^L xS_j(T)dl} \xrightarrow{define} = \frac{S_i(T_{ij})}{S_j(T_{ij})} \quad (6)$$

where T_{ij} is defined to be the "average" temperature that would be found by *assuming uniform properties* across the path (Eq. 7):

$$T_{ij} = \left[\frac{1}{T_0} - \frac{1}{1.44(E_i-E_j)}\ln\left(R_{ij}\frac{S_{0j}}{S_{0i}}\right)\right]^{-1} \quad (7)$$

Because S is a nonlinear function of T, the integrals in Eq. (6) represent a nonlinear averaging process. This means that the ratio of the absorbances becomes a function of the two chosen lines. The average temperature T_{ij} will depend on the chosen line pair because each line has a different dependence on temperature. This result will also depend in great measure on the correlation between concentration and temperature. The more we know about how the mole fraction and temperature are related, the more meaningful T_{ij} becomes.

While no discrete spatial information can be obtained when using only one line of sight sensor, one can compute various "average" temperatures by measuring several pairs of lines. These different temperatures can yield information about the degree of temperature uniformity of the flow. As the temperature profile becomes uniform, these temperatures (T_{ij}) will converge to the same number. This fact can be used to measure the degree of nonuniformity in the flow. Previous work at Georgia Tech[7,8] used numerical simulation of water absorption using the HITRAN database. It was shown that with three appropriately chosen absorption lines one can monitor for the

presence of hot or cold spikes in the exhaust flow of a high-pressure combustor. A similar approach was later applied to measurements of O_2 profiles in static heated cells of air.[9] Many closely spaced absorption lines were measured and used to compute the mole fraction or column-density of O_2 corresponding to predefined temperature bins over the range of temperatures expected in the gas.

The more lines one can measure, the more information can be inferred about the temperature distribution along the line of sight.

III. Test Rig and Simulations Setup

A. Combustor Test Rig

In a previous paper[10] we described a first implementation of a temperature nonuniformity sensor in the exit of a stratified methane-air combustor. The combustor test rig had two injectors: a methane-air primary injector and a dilution air injector. Mixing or the two jets was difficult, allowing for little control authority over the exit temperature profiles. Furthermore, because of the flow configuration and heat losses, the combustor could not achieve high exhaust temperatures.

The rig was subsequently modified to provide higher temperature conditions and to allow for control authority over the temperature profile. This was achieved by distributing the dilution air uniformly around the primary methane-air injector. The modified experimental setup is presented in Fig. 2.

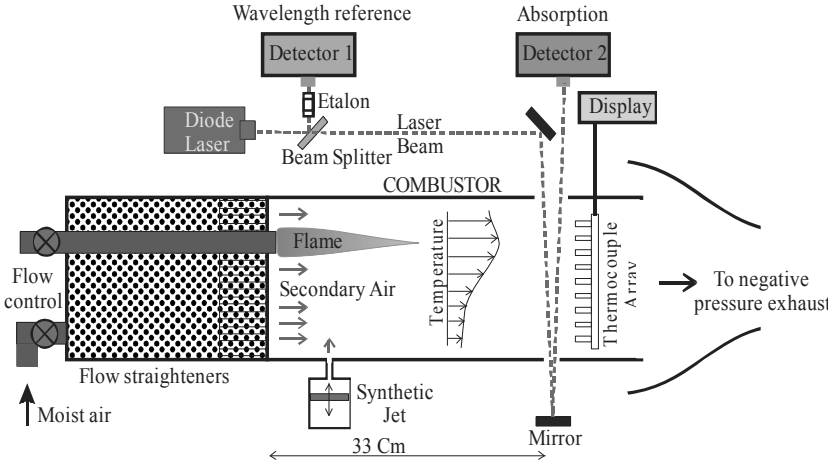

Figure 2. Combustor test rig.

The combustor has a rectangular cross-section (2"×3"). A primary methane-air injector is located near the top of the combustor. Secondary (dilution) air is injected through a region filled with glass balls and then through flow straighteners resulting in a parallel flow enveloping the primary injector. The flow rates of methane, primary, and secondary air can all be varied independently, but are generally adjusted such that the velocities of the primary injector and dilution air are close to each other. At the combustor exhaust, there is a vertical array of thermocouples just downstream of the laser path.

The exhaust temperature profile can be controlled in two ways. First, the relative flow rates of the primary and secondary air can be changed. In this case, the total water content of the exhaust is kept constant if the total air supply rate remains the same. Another way to change the temperature profile is to enhance mixing between the cold air stream and the flame products. In the current setup, this is accomplished with an array of synthetic jets[11,12].

A synthetic jet is a mixing actuator that requires no external mass flow. It typically consists of a cavity with a small orifice leading to the flow of interest. The cavity volume is modulated such that it sucks fluid from the flow field during its expansion and ejects it in a jet like manner during its compression. In our combustor it can move cold fluid from the bottom of the stratified combustor into the hot region above and provide cross-stream momentum to enhance the mixing. The mixing enhancement increases roughly with modulation frequency for our configuration, but at high frequencies the effects diminish[11,12].

The light source is a New Focus Velocity, external cavity tunable diode laser with a maximum power of 3.5 mW, operating over 1950–2040 nm. The laser beam passes through a beam-splitter, with one beam sent through an air-spaced etalon to an InGaAs detector used to monitor the relative wavelength. The second beam is double passed through the exhaust gases of the combustor with a second InGaAs detector used to measure the absorption of the beam at the combustor exhaust. The voltage signal from the two detectors is captured by a computer data acquisition system.

The external cavity diode laser used here has two tuning modes: a slow tuning mode over the full wavelength range of the laser; and a fast tuning mode (up to ~150Hz) over about 0.3 nm. A sample slow scan is shown in Fig. 3. The large (saw-tooth like) changes in laser power with wavelength are due to etalon effects in the laser cavity, and the small dips represent absorption lines. Measurement limitations arise because small changes in the absorption

lines have to be measured over large changes in the incident laser power. Moreover, because of the difficulty in accurately fitting a background and because of unsteadiness in the combustor, the slow tuning mode of this laser is more difficult to use for sensor measurements. The large change in laser power is characteristic for external cavity lasers. Most commercially available lasers (though often with smaller tuning range) have much better tuning characteristics and would likely result in better sensor performance.

Thus, we present data acquired using only fast tuning, despite its limited wavelength range. This limits our measurements to scanning over one line at a time. To obtain the three or more lines needed by the sensor, the laser is rapid tuned (~70 Hz, which produces 140 line scans/second) over one absorption line for one second or more, then the laser wavelength is slowly changed to a new line location and the fast scans are repeated. Since the lines are not captured at the same time, averages of multiple measurements are needed to decrease the effects of combustor unsteadiness and beam steering.

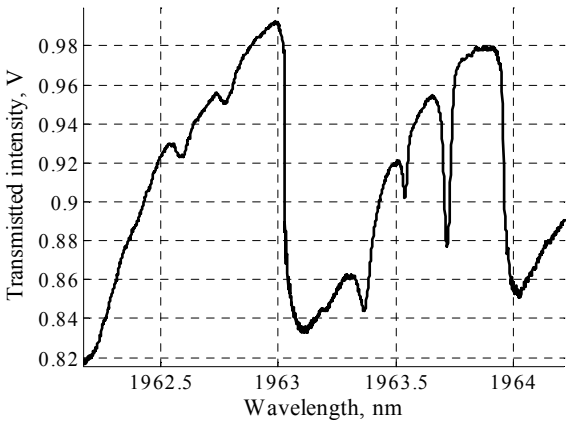

Figure 3. Slow laser tuning over a large wavelength range.

The detector signals must be corrected to produce accurate absorption measurements. One must account for the changes in laser intensity due to scanning (noted above), beam walk and beam steering, and background absorption due to water in the room air. To obtain an absorption measurement, regions far from the line center (e.g., the far wings of an isolated absorption line) are used to fit a polynomial background that gives the incident intensity (I_0). Measurements or room air absorption are taken before the combustor is started and later subtracted from all combustor absorption measurements.

B. CFD Data for Sensor Simulations

Because of limitations of the experimental setup, the sensor operation was also simulated for several combustor exit temperature and species profiles obtained from a Large Eddy Simulation (LES)[13] of a turbulent, axisymmetric, premixed, gas fueled, swirl-stabilized combustor with adiabatic walls operating at 6 atmospheres (Fig. 4). Exit temperatures are on the order of 1000-2000 K. Several instantaneous profiles at three downstream stations near the exit are used for the sensor simulations. These satiations are used to represent different combustor conditions. The absorbances of water lines along a diameter of the combustor are calculated for the given temperature and concentration profiles using spectroscopic data from the HITRAN 2004 database.

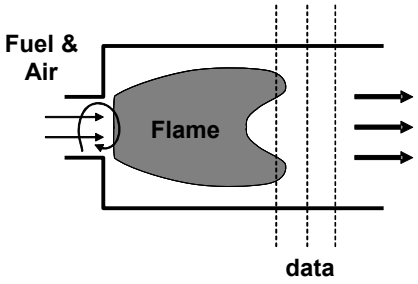

Figure 4. CFD combustor geometry.

IV. Sensor Concept and Operation

The sensor described here is intended to be part of a system for controlling temperature nonuniformity (pattern factor). It is desirable to have a simple output, ideally one variable that would increase with the degree of nonuniformity of the measured profile. Below we will define one such variable and show simulations of the sensor operation.

A. Measures of the Temperature Profile

For gas turbine engines, the combustor exit temperature profile is generally described by the pattern factor, which may be considered an indicator of the maximum thermal loading of the turbine blades and vanes. Nevertheless, the pattern factor is not an ideal control variable because it only captures the maximum of the temperature profile. Moreover, it is not a very good indicator of the shape of the temperature profile, neither the total extent of deviations from the mean temperature. For example a profile with 4 equal peaks above the mean and another one with just one peak will have the same PF, although traveling turbine blades will go through 4 sets of thermal gradients in the first case, and only one in the second. To better distinguish between such profiles, a new variable has to be defined that takes into account both the magnitude of the deviations as well as their widths, or the

diameter of these hot pockets. After considering the merits and shortcomings of several measures, we have decided to define a temperature profile factor (*Tpf*) using the rms over the mean of the combustor exit temperature (T_4) as a measure of its uniformity instead of using the pattern factor (Eq. 1).

$$Tpf = \frac{T_{4,rms}}{T_{4,average}} \tag{8}$$

The temperature profile factor is used in all the plots in the paper.

B. Nonuniformity Parameter

The sensor works by probing at least three water absorption lines with a laser. The absorptions of each pair of lines *i & j* yields a path-averaged temperature, T_{ij}, specific to the chosen pair. Two of these "average" temperatures are combined into a nonuniformity parameter 'U' defined below:

$$U = \frac{|T_{12} - T_{13}|}{0.5 \cdot (T_{12} + T_{13})} = \frac{\Delta T}{\overline{T}} \tag{9}$$

This variable goes towards zero when the gas has uniform properties, and increases as the temperature nonuniformity increases or as the degree of mixing decreases. As an example, *U* was computed for several simple temperature profiles with an average temperature of 1500 K and small deviations from the mean of 10% and 20% in temperature spanning 5% and 10% of the path (Fig. 5). The path length was chosen as 20 cm and water concentration was set to be constant for this comparison. As the size and extent of the temperature deviations increases, so does *U*.

The values of *U* in Fig. 5 are relatively small because the absorption lines chosen are not optimized for these temperatures. The sensitivity of *U* to small changes in the temperature profile depends mainly on the choice of absorption lines and their dependence on temperature. Ideally the three lines forming *U* should have very different dependence on temperature in the expected range. For example, one line could increase with temperature, one could decrease, and one could be relatively constant. The two pairs have to be chosen such that each has good sensitivity to temperature as well as relatively different slope or dependence on temperature.

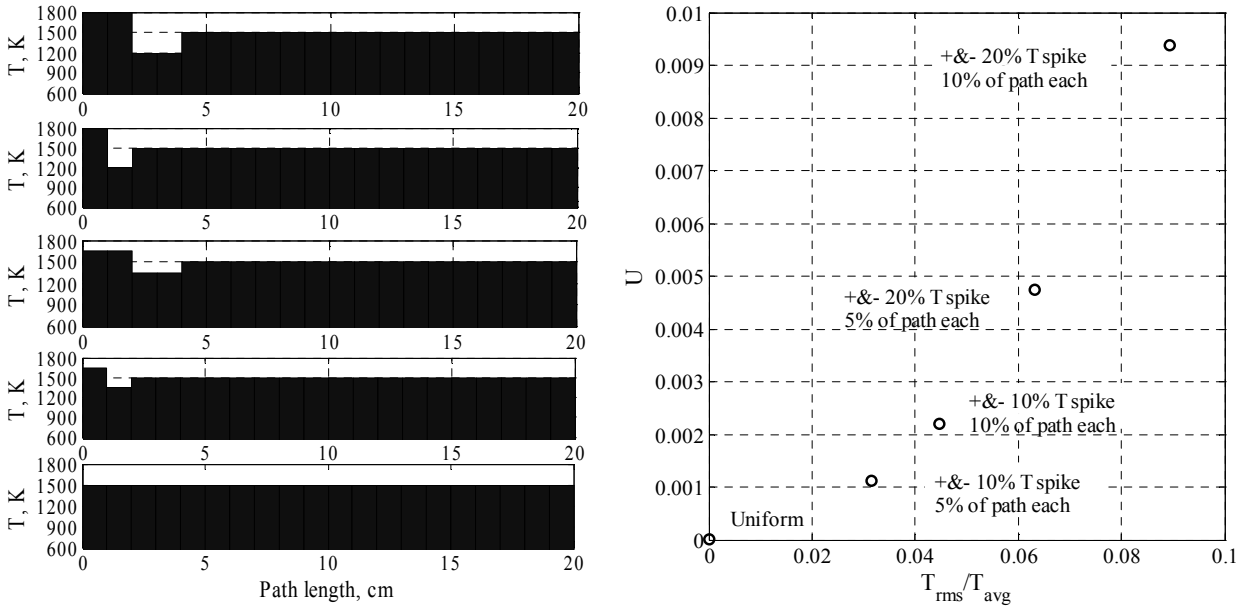

Figure 5. U values for several simulated temperature profiles with spikes of increasing magnitude and width. The water concentration was assumed constant.

V. Experimental Results

Results from initial measurements described in Ref. 10, demonstrated the ability of *U* to track changes in the temperature profile. This parameter was shown to decrease as the temperature along the line of sight became more uniform. Figure 6 shows *U* values for two temperature profiles obtained by changing the air distribution in the combustor. The *U* values for the more uniform profile (black squares) are smaller than for the profile with larger temperature swings (triangles).

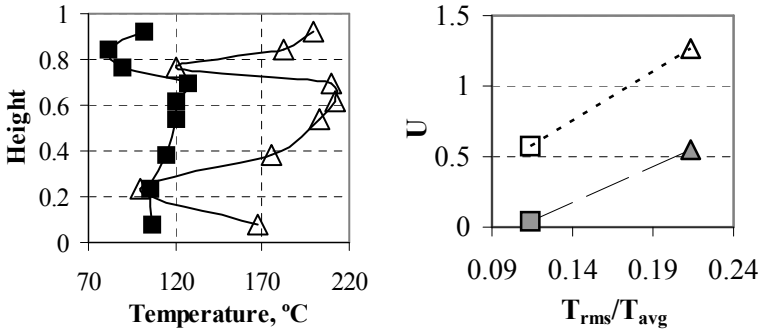

Figure 6. Combustor exit temperature profiles (left) for two operating settings and nonuniformity parameter U (right) based on two groups of absorption lines (dotted line and dashed line).

Although promising, the initial experiments exhibited several limitations. First as noted above, the available laser system limited measurements to one absorption line at a time. This limited the *U* values to average measurements. Because of combustor unsteadiness each line might be measured at slightly different conditions. In addition, sensor sensitivity and noise rejection were severely limited by the available absorption lines in the laser wavelength range. Also as explained above, the combustor rig used in the initial experiments allowed for little control authority over the exit temperature profiles.

The test rig was improved as described in section III above; typical exit temperature profiles are shown in Fig. 7. As suggested, the new configuration increased the range of temperature nonuniformity in the combustor exhaust, as well as increasing the maximum exhaust temperatures. However, the exhaust temperatures are still much less than the adiabatic flame temperature based on the overall air and fuel flow rates. This is due to significant heat losses at the combustor walls.

Measurements in the modified setup yielded mixed results. In certain cases (Fig. 8 a), the *U* parameter exhibited the desired trend (increasing with T_{rms}/T_{avg}) except for a few bad points. In other cases there was a large scatter of the *U* values, which do not appear to correlate with the degree of temperature nonuniformity, as can be seen in Fig. 8 b. To improve the measurements and redesign the sensor for better performance, next, we identify, analyze, and describe ways to eliminate the possible causes of errors that resulted in the large experimental scatter.

The likely sources of error in *U* include: wall heat losses, which can alter the relationship between local temperature and water concentration, the time-averaging process employed because of the inability to scan fast over several absorption lines, and noise. Simulated species and temperature profiles obtained from the time-resolved LES results allow us to investigate each of these error sources independently and to develop possible improvements.

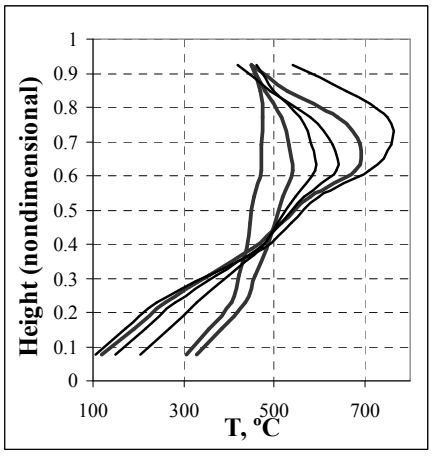

Figure 7. Typical combustor exit temperature profiles.

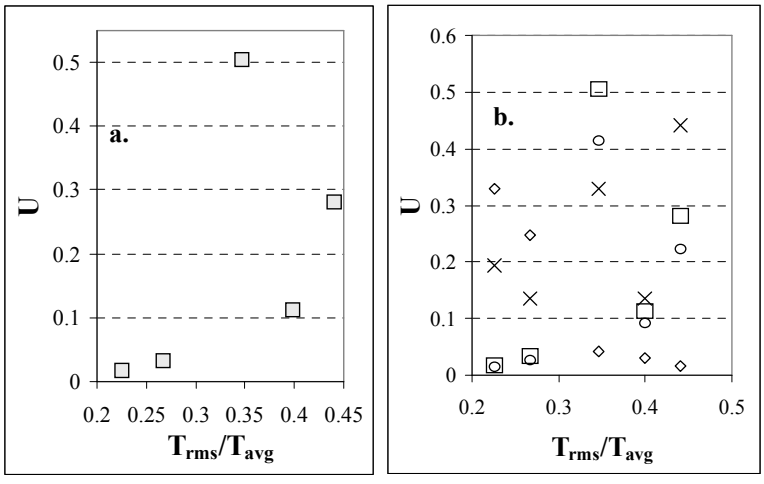

Figure 8. Measurements of U in the exit of a temperature stratified methane-air combustor.

VI. Sensor Simulation Results

A. Changing water-temperature correlation

As mentioned above, one of the possible reasons for the scatter in measured *U* values might be the changing correlation between water and temperature due to wall cooling in the test combustor. Any absorption sensor is affected both by the temperature field and the concentration field. If the temperature and concentration are correlated and the correlation never changes, it is equivalent to saying that the concentration is a set function of temperature, so that *U* will still be a measure of changes in the temperature profile only. When this correlation changes, than *U* becomes a composite measure of changes in the temperature field combined with "independent" changes in the concentration field. In most practical gas-turbine combustors the temperature and species concentrations are directly correlated (i.e. hotter regions have more water), regardless of operating conditions. Also, heat losses at the walls are relatively small.

In our combustor test rig, severe heat losses at the walls have a very large effect on the exit temperature profile, while the water mole fraction profile is relatively unaffected by the heat transfer. These losses greatly affect the spatial correlation between the species and the temperature field. As combustor operating conditions change, changes in wall cooling have larger effects on the temperature profile than on the absorber distribution. Effectively, this means that under different operating conditions, the local correlation between the temperature and species mole fraction may also be different. This changing relationship between temperature and species concentration has a large effect on *U*.

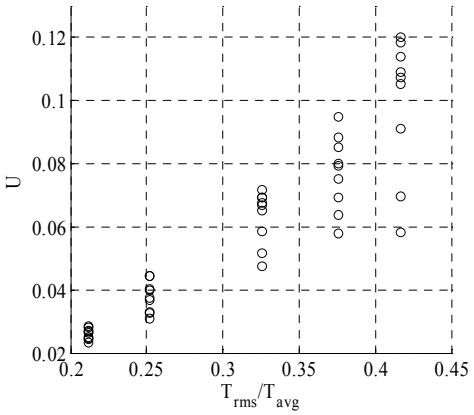

Figure 9. U for several correlations between temperature and concentration.

To investigate the effect of changes in correlation on *U*, we use the measured combustor exit temperatures (Fig. 7) and simulate the sensor operation for several water distributions at every operating condition. For example, for a given temperature profile characterized by a T_{rms}/T_{avg} value, we compute *U* for constant water, for water linearly dependent on temperature, quadratic, and several random water distributions with the same mean. The resulting *U* values for each operating condition (T_{rms}/T_{avg}) are shown in Fig. 9. Although the *U* values still increase overall, the resulting scatter becomes larger for less uniform profiles. If a single sequence is chosen, where the correlation is different at each operating condition, the resulting set of *U* values might show no obvious trend, as can be seen in Fig. 10. *U* is no longer monotonic and this effect can explain some of the results seen in Fig. 6.

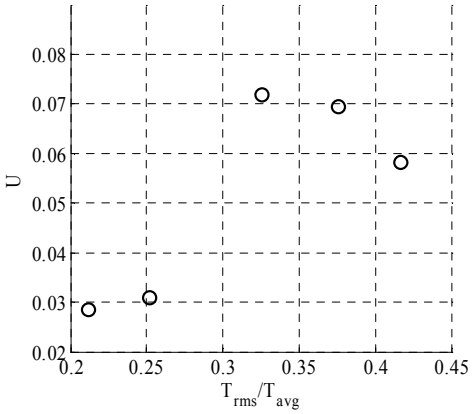

Figure 10. U when the correlation between temperature and concentration is different at each T_{rms}/T_{avg}.

Nevertheless, the *U* values and their scatter in these simulations are much smaller than the measured ones. Also small changes in correlation have a small effect on *U*. This suggests that the changing correlation is not a major problem and there are other factors, such as the inability to fast-tune the laser over several lines or noise that might have a larger contribution to the errors observed in the measured *U* values. Furthermore, this problem becomes even less significant for practical gas-turbine combustors where heat loses at the walls are small and large changes in correlation are not expected.

Because of limited experimental data and the inability to measure the water concentration in the test combustor we use CFD data as a tool to simulate the sensor and study the other possible sources of errors.

B. U for CFD profiles

The sensor performance is first simulated under ideal conditions (no noise and no sources of error) to validate the use of CFD data and to confirm that *U* is a sensible parameter for tracking nonuniformity under realistic combustor conditions. *U* is computed for several instantaneous temperatures (Fig. 11) and water mole fraction profiles from the CFD data. Because the combustor walls are adiabatic, water concentration is directly correlated with temperature. The resulting *U* values for each profile increase monotonically with T_{rms}/T_{avg} as shown in Fig. 12.

It should be noted that the values of *U* are relatively small: 0.035 means that the difference between the two temperatures composing *U* (Equation 9) represents a 3.5% deviation from their mean. For a mean temperature of 1500K this translates in a ΔT of 50K. For a given temperature profile, the size of this ΔT depends on the difference in temperature dependence between the two chosen line pairs that form *U*. A larger difference in temperature dependence allows measurements of smaller spikes in the temperature profiles as well as having better signal to noise ratio.

From Fig. 11 and 12 it can also be seen that *U* is monotonic with T_{rms}/T_{avg}. When used as an input to a control system, this means that driving down the value of *U* (through some means of actuation) results in a profile with smaller temperature extremes. Reducing the range of temperature extremes experienced by the turbine means the average burning temperature can be increased to improve engine efficiency.

Now we use the CFD data to analyze the other experimental shortcomings and their effect on *U*.

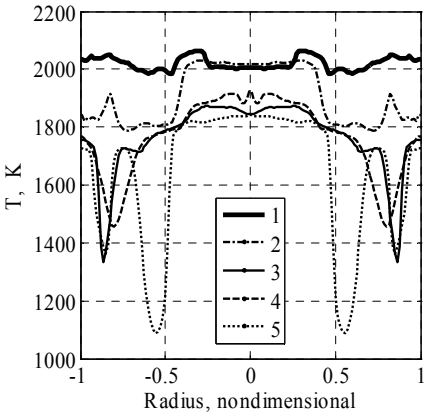

Figure 11. Exit temperature profiles for CFD data.

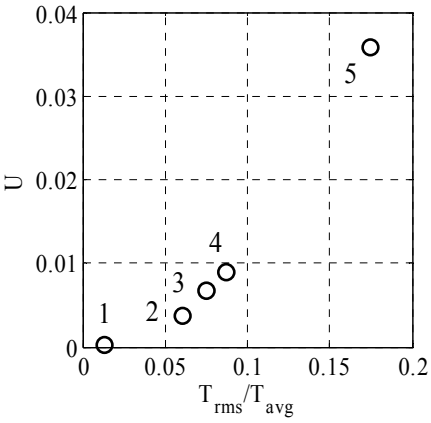

Figure 12. U based on CFD data.

C. Time-averaging

In the present experiments, the narrow fast tuning range of the laser limits measurements to one line at a time. Each line is measured for about two seconds, resulting in approximately 300 absorbance values. If the test combustor exhibits low frequency unsteadiness, it might not be captured in the two second scan for each line. Also, because the lines are not measured quasi-simultaneously, each line might be measured at a slightly different combustor condition. The resulting *U* value can be off by a large amount.

Absorption measurements for each line are averaged and then the averages are used to compute *U* for the "nominal" or average combustor conditions (set flow rates). Theoretically, the longer the time each line is measured, the more representative will the average be of the nominal operating conditions.

The simulations are used to determine if *U* based on the average of absorbances at the same nominal condition is still an indicator of the average temperature profile. Each of three nominal combustor operating conditions is represented by eight instantaneous temperature and water mole fraction profiles (Fig. 13) representative of temporal fluctuations in the combustor. Two situations are compared. First,

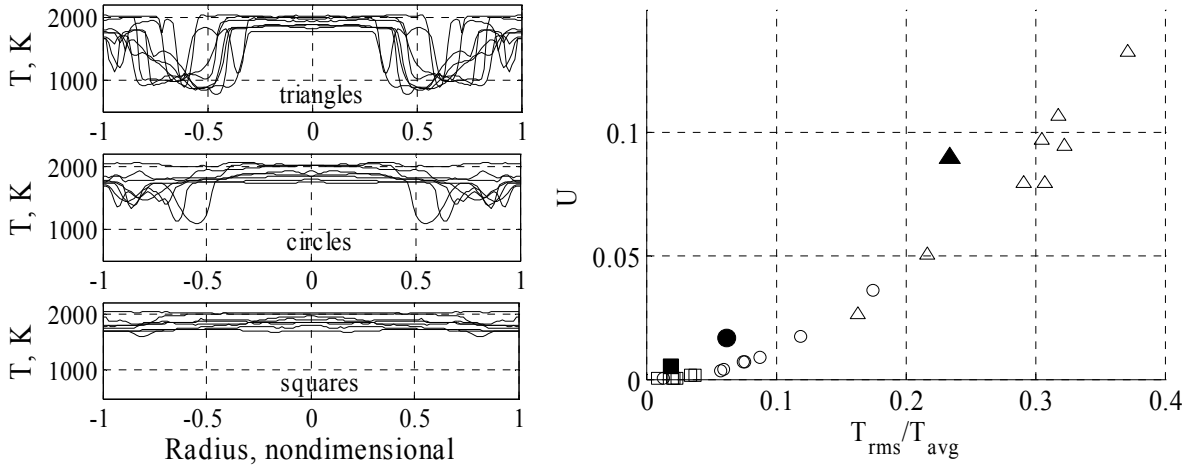

Figure 13. U for instantaneous (open symbols) and average (solid symbols) absorbances. Each set of instantaneous temperature profiles on the left correspond to a nominal combustor operating condition, denoted in the right plot by the same type of symbols.

instantaneous *U* values are computed for each of the eight profiles and are plotted versus the T_{rms}/T_{avg} of each of those profiles (Fig. 13 – open symbols). Because of the fluctuations, each nominal condition has a range of profiles, spanning a range of nonuniformities. All the instantaneous *U* values show a consistent increasing trend with T_{rms}/T_{avg}.

Second, *U* is computed for each nominal condition based on the average of the 8 instantaneous absorbance measurements. Practically, this assumes that all fluctuations are captured by the measurements of each line, equivalent to a very long average. The resulting *U* values (Fig. 13 – solid symbols) are plotted versus the T_{rms}/T_{avg} of the average temperature profile at each operating condition. These *U* values are representative of the average conditions and maintain the monotonic increase with average temperature nonuniformity, suggesting that there are no nonlinear effects affecting the averaging process. These simulations demonstrate that if the averaging is long enough and captures most of the fluctuations in the combustor, than the resulting *U* values have the desired dependence on average temperature nonuniformity.

So far we have shown that water-temperature correlation changes do not introduce very large errors in *U*, while the time-averaging process is good for providing information on average combustor temperature profiles. Neither of these potential problems introduced large fluctuations in *U* and neither resulted in the large *U* values observed in the experiments. This suggests that other factors introduce the dominant errors in *U*.

D. Noise

Measurement noise and errors are another major source of uncertainty for *U*. First, there are several sources of errors that can be eliminated through experimental redesign. For example random noise can be averaged out, absorption due to room air can be eliminated by using fiber optics or purging the air path with an inert gas, and etalon effects are reduced or eliminated by slanting the optics.

Another type of errors are random-type or symmetric errors which can be eliminated by averaging a large number of measurements. Combustor unsteadiness, turbulence, fluctuations in the air and fuel supply can usually be eliminated by taking a large number of scans over a long enough time to capture the average operating conditions. Also, fast tuning at kHz rates is needed to freeze most of these modes, such that the temperature and concentration profiles do not change during a single line scan.

Using the CFD data, we simulate this kind of experimental noise by adding a random error of up to ±1.5% of each absorbance value, similar to errors in the absorption measurements. Small errors in the absorbance values result in a large scatter of the instantaneous *U* values (Fig. 14). Nevertheless, average *U* values are still representative of the combustor temperature profile, with larger average *U* values corresponding to profiles with bigger temperature swings. Figure 14 illustrates that if enough data is taken, the random-type noise can be reduced by averaging. Choosing lines with good temperature sensitivity decreases the spread in *U* values resulting from the same level of errors in the measured absorbance.

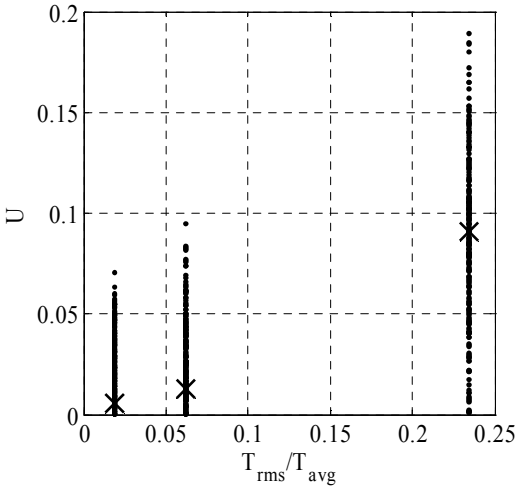

Figure 14. U based on noisy absorbances (dots) and U for the average of the absorbances (X).

However, this figure also shows that small errors in absorbance (1.5%) have a large effect on individual *U* values (±100%), which suggests that non-random errors (such as background fitting, room air absorption, etc.) that can not be averaged may be the main source of errors in the measured *U* values (Fig. 8). Some of the worst errors generally have a bias, such as consistently under-fitting the laser incident power (background). This background can be measured with a second detector or by fitting a curve through the far wings of an absorption line – as in our setup. Errors in fitting the right background are exacerbated by the fact that the laser power changes nonlinearly with wavelength, as shown in Fig. 3. Poor background fitting can introduce errors of a few percent of the integrated absorption. These errors are generally of a systematic manner, skewing the absorbance in one direction.

Beam steering is another major issue. Beam steering is the result of temperature gradients along the line of sight that change the index of refraction of the gas and results in the beam walking off the detector. If the time-scale of the beam steering is of the same order of magnitude as the time it takes to scan over one line, a bell-curve decrease in the detector signal is superimposed over the absorption signal, increasing the measured absorbance. Fast tuning (kHz

or better) can be used to essentially "freeze" the beam steering effects due to lower frequency combustor unsteadiness. Optical system design (focusing the laser beam, using collecting optics, etc.) can also decrease the beam steering effects. Other noise reduction techniques, such as 2f spectroscopy can also be used to eliminate some of these errors, such as background fitting, but at the cost of increased hardware and computational complexity.

In conclusion, through the simulations we showed that most of the source of errors (changing correlation, time-averaging, most symmetric noise) do not introduce large fluctuations in U. Furthermore, these errors can be mitigated by improving the experiment (using a laser with faster tuning ability, optical system redesign, and adding detectors for incident laser power and room air absorption). There remain however a few sources of errors, such as laser background fitting or beam steering that could still have a significant impact on sensor performance. If care is taken in the sensor design, most shortcomings can be overcome and a sensor suitable for pattern factor control can be constructed.

VII. Extension to Temperature Distribution Sensing

The simulation data also allows us to investigate other techniques for obtaining information about the combustor exit temperature. There are situations (e.g. for testing or combustor development) when we want to know more about the temperature profile, for example the mean temperature, the relative magnitude of the deviations from the mean, etc. A technique for providing more information about the shape of the temperature profile was developed in Ref. 9.

By measuring several absorption lines (the more the better) and choosing a set of temperatures expected in the flow, one can compute a relative "amount" of gas in each of these predefined temperature bins from the measured absorbances. More specifically, the following equation can be used:

$$S_{ij}(xL)_i = abs_j \tag{10}$$

where S_{ij} is the matrix of line strengths of line j at predefined temperature T_i, $(xL)_i$ is the column-density (mole fraction times length) of water at temperature T_i, and abs_j is the measured absorbance of line j. The result is a histogram type plot of the amount of water at each chosen temperature. The temperatures T_i can be selected iteratively, starting with a wide range and reducing it until most bins have a positive contribution. The more lines and the fewer temperature bins, the better the results. These plots give much more information than U about the exit temperature distribution along the line of sight.

Using seven absorption lines we compute the water column density corresponding to the temperature profiles shown in Fig. 11. The resulting histograms are shown in Fig. 15. For the most uniform temperature profile, the first histogram shows that most of the water is distributed around 1756 ºC, the weighted average of the two bars. The first two histograms, corresponding to the more uniform profiles, show that the water is generally distributed in a relatively narrower temperature band than the other three cases. The most nonuniform profile has the last histogram with the largest spread. This process can be used instead of U to better understand the temperature profile.

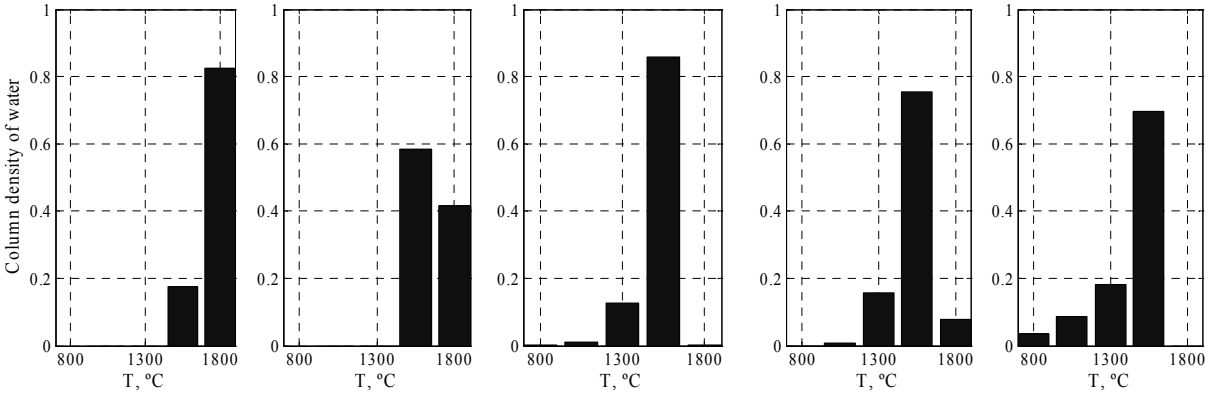

Figure 15. Histograms of exit temperature profiles based on 3 absorption lines.

VIII. Conclusions

Experimental tests of a sensor for controlling temperature nonuniformity in the exit of a combustor were presented. The sensor is based on line-of-sight absorption of multiple absorption lines, and an output parameter, *U*, is shown to generally correlate with the degree of temperature nonuniformity, T_{rms}/T_{avg}. Although initial results were promising, further experimental testing revealed several problems when measuring the nonuniformity parameter *U*. The likely sources were identified to be the changing correlation between concentration and temperature in a combustor with significant heat losses, the inability to scan all the absorption lines in a short time, and noise. Sensor simulations were successfully used to investigate these problems. While the effects of heat losses were significant in the current combustor, the variation in the water-temperature correlations are not significant in gas-turbine combustors and can also be ameliorated by choosing absorption lines with better temperature sensitivity. Fast tuning limitations that result in time-averaging issues can be solved by using better lasers, or by taking long enough averages to capture most of the combustor unsteadiness. Finally, the influence of experimental noise on *U* can be significant, but it can be decreased to acceptable levels through averaging and other noise reduction techniques.

In conclusion, a simple nonuniformity sensor for pattern factor control can be constructed if care is taken to decrease the above sources of errors and if appropriate hardware is used. The application of the histogram technique to study the temperature profile in a combustor exit is also introduced.

IX. Acknowledgments

This research was performed under the support of a NASA University Research, Engineering, and Technology Institute (URETI) grant on Aeropropulsion and Power.

X. References

[1] Teichert, H., Fernholz, T., and Ebert V., "Simultaneous in situ measurement of CO, H2O, and gas temperatures in a full-sized coal-fired power plant by near-infrared diode lasers," *Applied Optics*, Vol. 42, No. 1220, April 2003, pp. 2043-2051.

[2] Allen, M.G., "REVIEW ARTICLE: Diode laser absorption sensors for gas-dynamic and combustion flows," *Measurement Science and Technology*, Vol. 9, 1998, pp. 545–562.

[3] Zhou, X., Liu, X., Jeffries, J.B., and Hanson R.K., "Development of a sensor for temperature and water concentration in combustion gases using a single tunable diode laser," *Measurement Science and Technology*, Vol. 14, 2003, pp. 1459–1468.

[4] Mihalcea, R.M., Baer, D.S., Hanson, R.K., "Diode-laser absorption measurements of CO_2 near 2 μm at elevated temperatures," Applied Optics, Vol. 37, No. 36, 20 December 1998, pp. 8341-8347.

[5] Nagali, V. and Hanson, R.K., "Design of a diode-laser sensor to monitor water vapor in high-pressure combustion gases," *Applied Optics*, Vol. 36, No. 36, 20 December 1997, pp. 9518-9527.

[6] Rothmana, L.S., Barbeb, A., Chris Bennerc, D., Brownd, L.R., Camy-Peyrete, C., Carleerf, M.R., Chancea, K., Clerbauxf, C., Danae, V., Devic, V.M., Fayth, A., Flaudi, J.M., Gamachej, R.R., Goldmank, A., Jacquemarta, D., Jucksa, K.W., Laffertyl, W.J., Mandine, J.-Y., Massiem, S.T., Nemtchinovn, V., Newnhamo, D.A., Perrini, A., Rinslandp, C.P., Schroederq, J., Smitho, K.M., Smithp, M.A.H., Tangq, K., Tothd, R.A., Vander Auweraf, J., Varanasin, P., Yoshinoa, K., "The HITRAN molecular spectroscopic database: edition of 2000 including updates through 2001," *Journal of Quantitative Spectroscopy & Radiative Transfer*, Vol. 82, 2003, pp. 5–44.

[7] Seitzman, J.M. and Scully, B.T., "Broadband infrared absorption sensor for high-pressure combustion control," *Journal of Propulsion and Power*, Vol. 16, No. 6, pp. 994-1001, 2000.

[8] Seitzman, J.M., Tamma, R., and Scully, B., "Broadband infrared sensor for active control of high pressure combustors," AIAA Paper 98-0401, *Aerospace Sciences Meeting & Exhibit*, 36th, Reno, NV, Jan. 12-15, 1998.

[9] Sanders, S.T., Wang, J., Jeffries, J.B., and Hanson, R.K., "Diode-laser absorption sensor for line-of-sight gas temperature distributions," *Applied Optics*, Vol. 40, No. 24, 20 August 2001, pp. 4404-4415.

[10] Palaghita, T. and Seitzman, J. M., "Control of temperature nonuniformity based on line-of-sight absorption," AIAA Paper 2004-4163*, AIAA/ASME/SAE/ASEE Joint Propulsion Conference and Exhibit, 40th,* Fort Lauderdale, FL, 11 - 14 Jul 2004.

[11] Chen, Y, Liang, S, Aung, K, Glezer, A, Jagoda, J, "Enhanced mixing in a simulated combustor using synthetic jet actuators," AIAA Paper 99-0449, *Aerospace Sciences Meeting and Exhibit*, 37th, Reno, NV, Jan. 11-14, 1999.

[12] Chen, Y, Scarborough, D, Liang, S, Aung, K, Jagoda, J, "Manipulating pattern factor using synthetic jet actuators," AIAA Paper 2000-1023, *Aerospace Sciences Meeting and Exhibit*, 38th, Reno, NV, Jan. 10-13, 2000.

[13] Eggenspieler, G. and Menon, S, "Parallel Numerical Simulation of Flame Extinction and Flame Lift-Off," Proceedings of the *Parallel Computational Fluid Dynamic Conference*, Washington, DC, May 24-27, 2005